Chapter 15
Solar Assisted Organic Rankine Cycle for Power Generation: A Comparative Analysis for Natural Working Fluids

Önder Kizilkan, Sandro Nižetić, and Gamze Yildirim

Introduction

The steam Rankine cycle is one of the most important ways to transform on large scale thermal energy into power. Because of its good properties, water is the most suitable working fluid for high temperature applications and large centralized systems. Seeking for small and medium scale power plants, the problems encountered with water can be partially mitigated by selecting an appropriate fluid. Organic compounds characterized by higher molecular mass and lower critical temperature than water have been proposed in so called Organic Rankine Cycles (ORC) (Tchanche et al. 2011). ORC, as a method of low grade heat utilization can rise the energy utilization by conversion of heat into electric energy (He et al. 2012). There are lots of low temperature practices in which the ORC can be used such as solar thermal, biomass geothermal oceanic, waste heat from power plants, combined heat and power, waste heat from industrial processes, etc. (Peris et al. 2015).

The development of solar assisted power plants is becoming more crucial because of effects of fossil fuels. For this reason, there is a need to improve existing technologies integrated with solar energy. These systems offer better advantages

Ö. Kizilkan • G. Yildirim (✉)
Department of Energy Systems Engineering, Faculty of Technology, Süleyman Demirel University, 32200 Isparta, Turkey
e-mail: onderkizilkan@sdu.edu.tr; gazmeyildirim@sdu.edu.tr

S. Nižetić
Department of Thermodynamics and Heat Engines, Faculty of Electrical and Mechanical Engineering and Naval Architecture, University of Split, R. Boskovica 32, 21000 Split, Croatia
e-mail: snizetic@fesb.hr

P. Grammelis (ed.), *Energy, Transportation and Global Warming*, Green Energy and Technology, DOI 10.1007/978-3-319-30127-3_15

when compared traditional energy sources. Parabolic trough solar collector (PTSC) technology is considered the most established solar thermal technology for power generation. Therefore, this technology has been chosen for this study (Al-Sulaiman 2013).

Organic Rankine Cycle (ORC) as a promising energy transformation technology has been the focus of many investigators (Kerme and Orfi 2014). Over the last decades, significant researches have been carried out in the field of ORC systems. Dai et al. (2009) studied ORC for low grade waste heat recovery using various fluids. They examined thermodynamic parameters of the ORC for every working fluid. They concluded that the cycle with R236EA had the highest exergy performance. He et al. (2012) recommend a theoretical model to check out optimal evaporation temperature of subcritical ORC. In a different study, organic Rankine cycle and supercritical Rankine cycle for the transformation of low-grade heat into electrical power investigated by Chen et al. (2010). They analysed 35 different fluids for two cycles and analysed the effects of the selected fluid characteristics on the cycle performance. Wang et al. (2013) conducted a regenerative ORC to make use of the solar energy over a low temperature series. They used flat-plate solar collectors to collect the solar radiation for their low costs. Lee et al. (2012) investigated the impact of changing the proportion of the cooling water to the condenser on the performance of the ORC. They used R245fa in their analysis. Shengjun et al. (2011) studied performance comparison of the fluids in subcritical and transcritical ORC power cycle in 80–100 °C binary geothermal power system. They conducted the analyses with a program in MATLAB for thermal efficiency, exergy efficiency, recovery efficiency, heat exchanger area and levelized energy cost. Thermodynamic optimization of ORCs for power generation combined heating and power from different average heat source profiles researched by Maraver et al. (2014). Vélez et al. (2011) investigated the use of a low temperature heat source for power generation a carbondioxide transcritical power cycle theoretically. They reported that the efficiency have been increased by the use of an additional internal heat exchanger. Franchini et al. (2013) carried out simulations to estimate the performance of a solar Rankine Cycle and an integrated solar combined cycle. They combined the system with two different solar field configurations based on parabolic trough and power tower systems.

In this study, solar energy driven ORC is investigated thermodynamically for different natural refrigerants. For collecting the solar energy, PTSCs are used because of their good advantages. For the analyses of ORC, eight natural working fluids and a HFC type fluid are considered including, R170 (ethane), R1270 (propylene), R600 (butane), R600a (isobutene), R717 (ammonia), R744 (carbondioxide), R161 (fluoroethane), R218 (octofluoropropane), and a HFC type fluid, R134a. Analyses are made to examine the system performances energetically and exergeticaly. An attempt is also made to evaluate the exergy destruction rates in order to determine how to improve the process. Furthermore, a comprehensive performance assessment of the integrated system is conducted through parametric analysis to investigate the effects of changing operating conditions on the system efficiencies.

Natural Refrigerants and System Description

Natural refrigerants provide alternatives to a number of HCFC, CFC and HFC type refrigerants in addition to their zero ozone depletion potential (ODP) and low or no global warming potential (GWP) (Bolaji and Huan 2013). They are naturally occurring substances, such as hydrocarbons, ammonia, carbon dioxide, water and air. These substances can be used as cooling agents (heat transfer medium) in refrigerators and air conditioners (Refrigerants naturally 2015).

The general properties of the previously mentioned working fluids are given in Table 15.1 (ASHRAE 2004; Restrepo et al. 2008; Calm and Hourahan 2011). In the table, critical properties of the fluids are obtained using EES software (F-Chart 2015). As seen from the table, the selected natural refrigerants have zero ODP and relatively very small GWP values excluding R218 and R134a. Additionally, their atmospheric life times are relatively short. In spite of this, it must be noted that some natural refrigerants such as R170, R1270, R600, R600a and R161 are in A3 safety group which means they are highly flammable. Besides, R744, R218, R134a are belonged to A1 group that means they are non-flammable. The last fluid, R717, is in the lower flammability group with higher toxicity.

The ORC consists of four compounds: a turbine, an evaporator, a condenser and a pump. Required heat energy for the evaporator of the ORC is supplied by means of PTSCs. Therminol-VP1 is for the PTSC system as the heat transfer fluid (HTF), for its good heat transfer properties and good temperature control (Therminol 2014). Because of its good properties, it is used in many high temperature applications driven by PTSC such as power plants (Kumar and Reddy 2009; Vogel et al. 2014; Cheng et al. 2012; Al-Sulaiman 2014). The system operates as follows: The liquid organic working fluid from condenser is compressed by the pump and fed back to the evaporator, where it is heated by the useful heat delivered by the solar PTSCs, and becomes superheated vapor. The superheated vapor then enters to the turbine and expands to a low pressure. Subsequently, the turbine exhaust is intensified to liquid in the condenser by extracting heat to the environment and the cycle completes when the fluid is compressed by the pump. The schematic representation of the system and the T–s diagrams of the case study are given in Figs. 15.1 and 15.2 respectively.

In Fig. 15.2, there are two T–s diagrams, where the first one is for subcritical and the second one is transcritical cycle. In subcritical cycle, the system properties are under the critical values and in transcritical cycle, the heat absorption process takes place above the critical values where heat rejection process takes place below the critical values. For the second case, the gas heater placed instead of evaporator.

Table 15.1 Properties of the selected working fluids

ASHRAE number	Molecular formula	Critical pressure (kPa)	Critical temperature (°C)	Safety group	ODP (relative to R11)	GWP (relative to CO_2)	Atmospheric life time (year)
R170	CH_3CH_3	4872.2	32.172	A3	0	20	0.21
R1270	$CH_3CH{=}CH_2$	4664.6	92.420	A3	0	3	0.001
R600	$CH_3CH_2CH_2CH_3$	3796.0	151.975	A3	0	20	0.018
R600a	$CH(CH_3)_3$	3640.0	134.667	A3	0	20	0.019
R717	NH_3	11,333	132.25	B2	0	0	0.25
R744	CO_2	7377.3	30.98	A1	0	1	120
R161	CH_3CH_2F	5.09	102.20	A3	0	12	0.18
R218	$CF_3CF_2CF_3$	2.6	71.95	A1	0	8830	2600
R134a	CH_2FCF_3	4059.0	101.030	A1	0.000015	1410	14

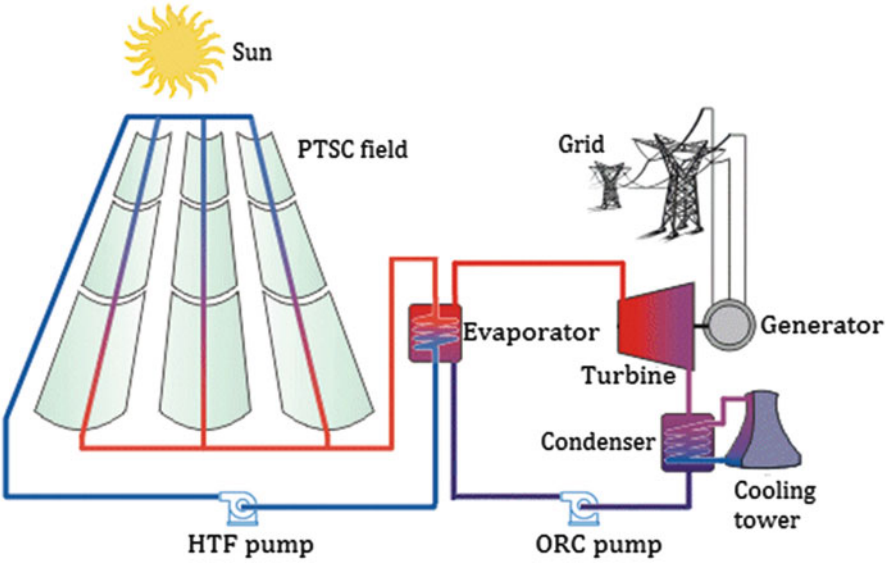

Fig. 15.1 Schematic representation of solar assisted ORC system (modified from Volker 2015)

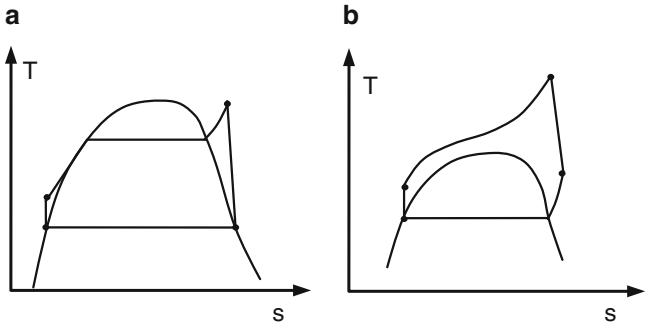

Fig. 15.2 T–s diagrams for ORC (**a**) subcritical (**b**) transcritical

Thermodynamic Analysis

The performance of the solar driven ORC is mathematically modelled using mass, energy and exergy balance equations. Some assumptions are made in order to find the work and heat interactions, the rate of exergy destructions, and the energy and exergy efficiencies. These are as follows:

- All the processes in the system are steady state and steady flow.
- The changes in potential and kinetic energies are neglected.
- The turbine and pumps are adiabatic.
- The heat transfer to/from ambient and pressure drops in the pipes are neglected.

- The natural fluid at pump inlet is saturated liquid.
- The dead state pressure and temperature are taken to be $P_0 = 101.325$ kPa and $T_0 = 25$ °C.
- The pinch point temperature of the evaporator and condenser/gas heater are taken as 10 °C (Al-Sulaiman 2014).

The general mass balance equation can be written as (Cengel and Boles 2006):

$$\sum \dot{m}_{in} = \sum \dot{m}_{out} \tag{15.1}$$

where m is the mass flow rate, subscripts in and out are entering and exiting streams to and from the system, respectively.

The general energy balance

$$\sum \dot{E}_{in} = \sum \dot{E}_{out} \tag{15.2}$$

For steady-flow processes the general energy balance can be written in more detail as:

$$\dot{Q} + \sum \dot{m}_{in} h_{in} = \dot{W} + \sum \dot{m}_{out} h_{out} \tag{15.3}$$

In above equations, E_{in} is the ratio of net energy transfer to the system, E_{out} is the ratio of net energy transfer from the system, Q is the ratio of net heat, W is the ratio of net work, and h is the specific enthalpy.

The rate of useful energy delivered by solar collector is (Tiwari 2003; Kalogirou 2009)

$$\dot{Q}_u = F_R[SA_a - A_r U_L(T_i - T_0)] \tag{15.4}$$

$$\dot{Q}_u = \dot{m} c_p (T_0 - T_i) \tag{15.5}$$

where F_R is the heat removal factor, S is the solar irradiation, A_a is the aperture area, A_r is the receiver area, U_L is the overall heat loss coefficient of solar collector, subscripts i, o and 0 are inlet, outlet and dead state, respectively.

The heat removal factor, F_R can be calculated from (Kalogirou 2009)

$$F_R = \frac{\dot{m} C_p}{A_r U_L}\left[1 - \exp\left(\frac{-A_r U_L F'}{\dot{m} C_p}\right)\right] \tag{15.6}$$

where F' is the collector efficiency factor and given by

$$F' = \frac{U_0}{U_L} \tag{15.7}$$

In Eq. (15.7), U_0 is the overall heat transfer coefficient. Based on PTSC properties, U_0 and U_L can be determined from (Kalogirou 2009):

$$U_0 = \left[\frac{1}{U_L} + \frac{D_o}{h_f D_i} + \left(\frac{D_o \ln\left(\frac{D_o}{D_i}\right)}{2k}\right)\right]^{-1} \tag{15.8}$$

$$U_L = \left[\frac{A_r}{(h_{c,c-a} + h_{r,c-a})A_g} + \frac{1}{h_{r,r-c}}\right]^{-1} \tag{15.9}$$

In above equations, $h_{c,c\text{-}a}$ is the convection heat loss coefficient between ambient and the cover, $h_{r,c\text{-}a}$ is the radiation heat transfer coefficient for the glass cover to the ambient, $h_{r,r\text{-}c}$ is the radiation heat transfer coefficient between the receiver tube and the glass cover and h_f is the heat transfer coefficient of fluid inside the tube. Additionally, D is the tube diameter and A_g is the glass cover area. The definitions of heat transfer coefficients mentioned above can be found in reference Kalogirou (2009) in more detail.

The general exergy balance equation can be defined as (Dincer and Rosen 2007):

$$\sum \dot{E}x_{in} = \sum \dot{E}x_{out} + \sum \dot{E}x_{dest} \tag{15.10}$$

The exergy balance equation can be expressed more explicitly as:

$$\dot{E}x_Q - \dot{E}x_W - \sum \dot{m}_{in} e_{in} - \sum \dot{m}_{out} e_{out} + T_0 \dot{S}_{gen} \tag{15.11}$$

where, Ex_Q and Ex_W terms are the exergies of heat and work, e is the specific exergy, T_0 is the dead state temperature and S_{gen} is the rate of entropy generation. The exergy terms in Eq. (15.11) are described below (Dincer and Rosen 2007):

$$\dot{E}x_{dest} = T_0 \dot{S}_{gen} \tag{15.12}$$

$$\dot{E}x_Q = \dot{Q}\left(\frac{T - T_0}{T}\right) \tag{15.13}$$

$$\dot{E}x_W = \dot{W} \tag{15.14}$$

The specific exergy can be expressed as (Cengel and Boles 2006; Bejan 1997):

$$e = (h - h_0) - T_0(s - s_0) \tag{15.15}$$

where, s is entropy, and subscript 0 stands for dead state properties.

The exergy of the solar radiation in terms of reference and sun's temperature is given by Petela (2005):

$$\dot{E}x_{solar} = SA_a\left(1 + \frac{1}{3}\left(\frac{T_0}{T_{sun}}\right)^4 - \frac{4}{3}\left(\frac{T_0}{T_{sun}}\right)\right) \tag{15.16}$$

where T_{sun} is the temperature of sun's surface and assumed as 5739 K (Tiwari 2003).

The energy and exergy efficiencies are described below (Dincer and Rosen 2007):

$$\eta = \frac{\dot{W}_{ORC}}{\dot{Q}_E} \tag{15.17}$$

$$\eta_{ex} = \frac{\dot{E}x_{out}}{\dot{E}x_{in}} = 1 - \frac{\dot{E}x_{dest}}{\dot{E}x_{in}} \tag{15.18}$$

Results and Discussion

For the thermodynamic analyses of the solar driven ORC, the system parameters for baseline conditions are given in Table 15.2. System characteristics of solar assisted ORC Table 15.2.

Using the general balance equations given in previous section, the analyses were made for the base line conditions first. According to data given in Table 15.2, the turbine power generations for different working fluids are given in Fig. 15.3.

Table 15.2 System characteristics of solar assisted ORC

PTSC system (Al-Sulaiman 2014; Kalogirou 2009)	Pipe receiver inner diameter	0.04 m
	Pipe receiver outer diameter	0.05 m
	Glass cover diameter	0.09 m
	Total length of PTSC	50 m
	Mass flow rate of HTF	0.32 kg/s
	Receiver emissivity	0.92
	Glass cover emissivity	0.87
	Temperature of the sun	5739 K
	Absorbed solar radiation	500 W/m^2
	Wind velocity	5 m/s
ORC	Turbine isentropic efficiency	0.85
	Pump isentropic efficiency	0.90
	Evaporator temperature[a]	50 °C
	Condenser temperature	27 °C
	Turbine inlet temperature	150 °C

[a]Turbine inlet pressure of ORC is determined from saturation pressure corresponding to evaporator temperature excluding R170 and R744, since the critical properties of these fluids are below from the specified values

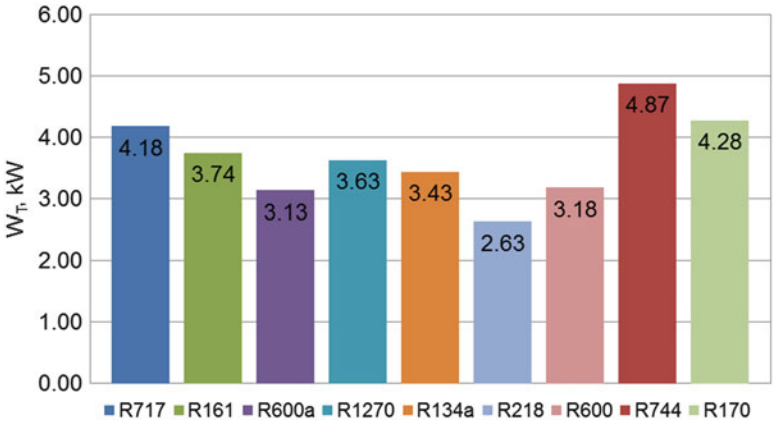

Fig. 15.3 Comparison of net power generation for different natural refrigerants

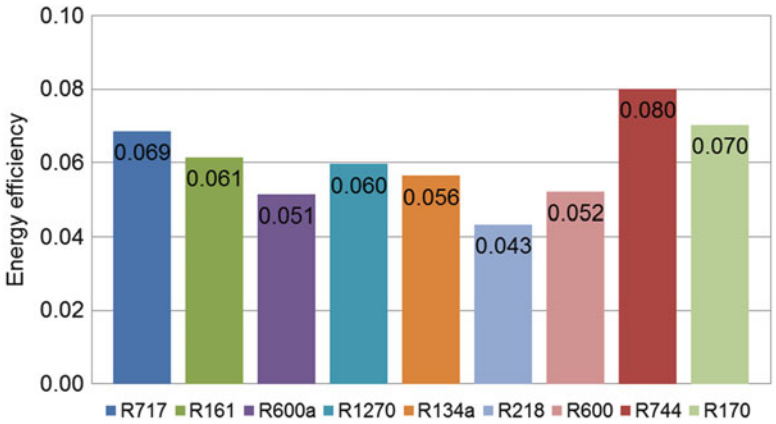

Fig. 15.4 Comparison of energy efficiencies of ORC for different natural refrigerants

As seen from the figure, ORC working with R744 has the highest power generation capacity and followed by R170, R717 and R161.

Figures 15.4 and 15.5 show the energy and exergy efficiencies of ORC for different working fluids according to the energy and exergy analysis. As seen from Fig. 15.4, the best energy performance is obtained using R744 with an energy efficiency of 8 %, whereas the lowest energy efficiency belongs to R218 with an efficiency rate of 4.3 %. The exergy efficiency results show that the highest efficiency is found to be 7.1 % with R744 and followed by R170 and R717.

A comparison of the calculated exergy destruction rates of the solar assisted ORC is given in Fig. 15.6. As seen from the figure, R218 has the highest exergy destruction rate and followed by R600a, R600 and R134a. The lowest exergy destruction rate is found to be 75.33 kW using R717.

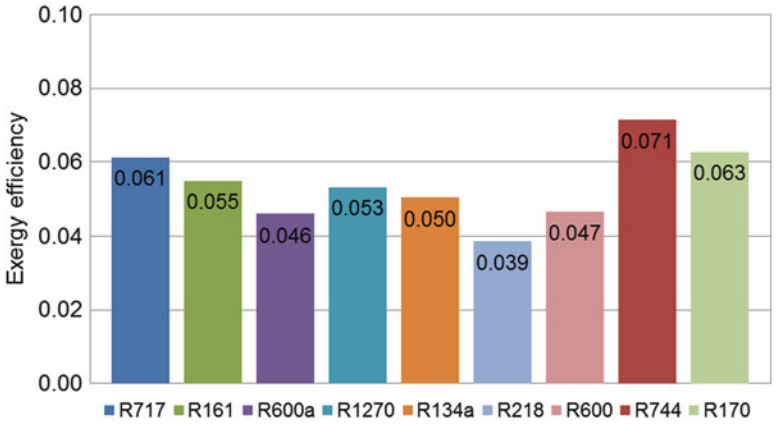

Fig. 15.5 Comparison of exergy efficiencies of ORC for different natural refrigerants

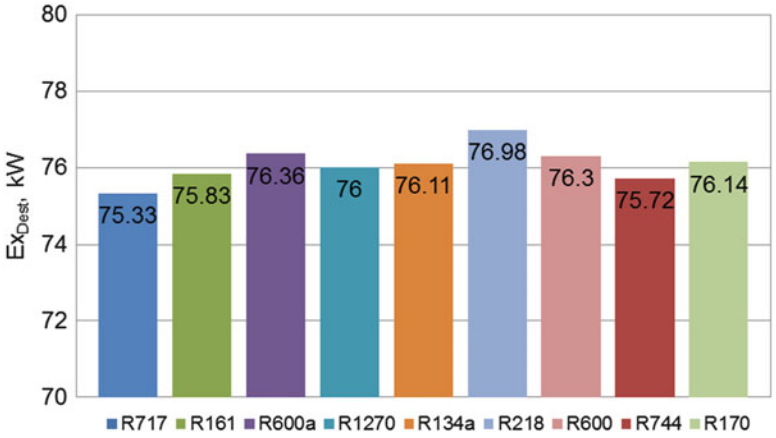

Fig. 15.6 Comparison of exergy destruction rates of ORC for different natural refrigerants

In Fig. 15.7, exergy destruction in the heat transfer process between the HTF and the working fluid in the evaporator is given. As mentioned earlier, Therminol-VP1 was used as HTF and its properties were kept constant during the calculations. Therefore, the differences between exergy destruction of evaporator is mainly depends on the working fluid properties. From the figure, it can be seen that the lowest exergy destruction rate in the evaporator is found to be 16.55 for R170, followed by R218 and R744 where evaporator of R717 has the highest exergy destruction with 19.41 kW.

Through parametric analyses, a comprehensive performance assessment of the integrated system was conducted to investigate the effects of varying operating conditions on the system efficiencies. For the parametric analyses, the variable parameters were selected to be solar radiation intensity, turbine inlet temperature,

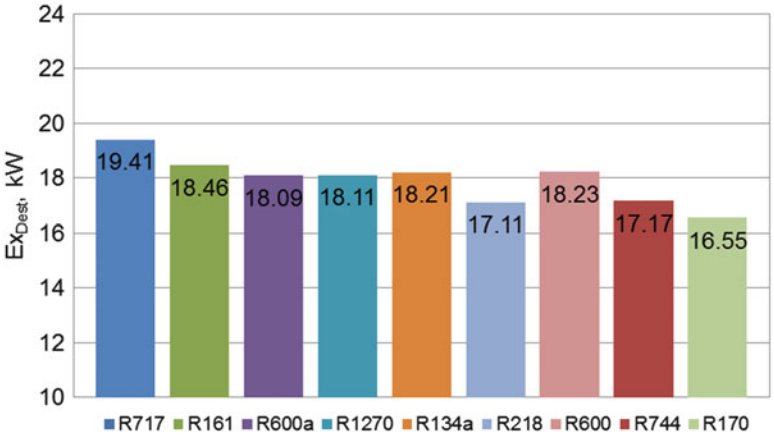

Fig. 15.7 Comparison of exergy destruction rates of evaporator for different natural refrigerants

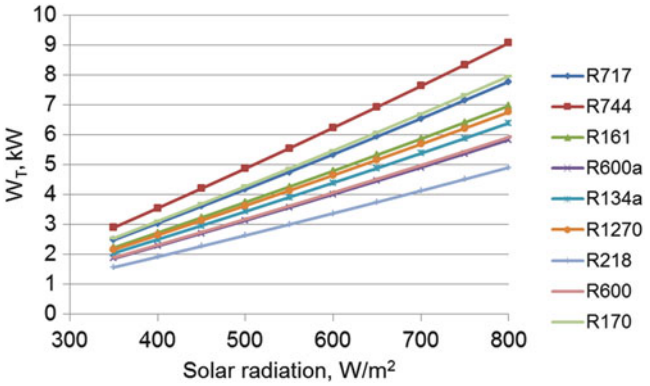

Fig. 15.8 Variation of net power generation with solar radiation

and normalized pressure at the turbine inlet and condenser temperature. Figure 15.8 shows the variation of solar radiation intensity with turbine power generation. As seen from the figure, turbine power generation increases with increase of solar radiation from 350 to 800 W/m^2.

Turbine inlet temperature also affects the cycle performance characteristics. To determine the variation of turbine inlet temperature on energy and exergy efficiencies, it was varied between 70–150 °C (Figs. 15.9 and 15.10). As seen from the figures, with the increase of turbine inlet temperature, energy and exergy efficiencies increase for R717. For the working fluids R744, R170, R134a, R600, R600a and R218, the efficiencies decrease whereas they are not affected so much for R161 and R1210 with the temperature.

Figure 15.11 shows the variation of turbine inlet temperature with the total exergy destruction rate of the system. As seen from the figure, the trend is contrary

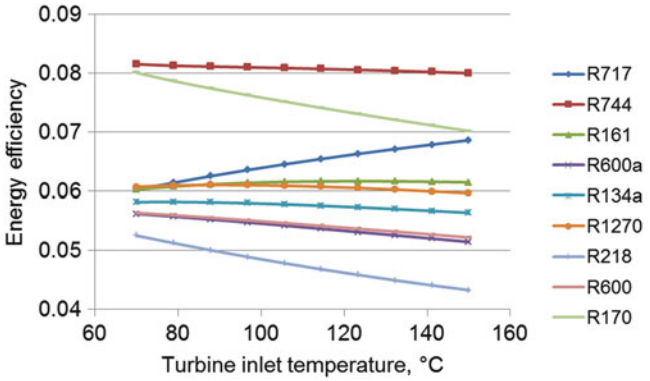

Fig. 15.9 Variation of turbine inlet temperature with energy efficiency

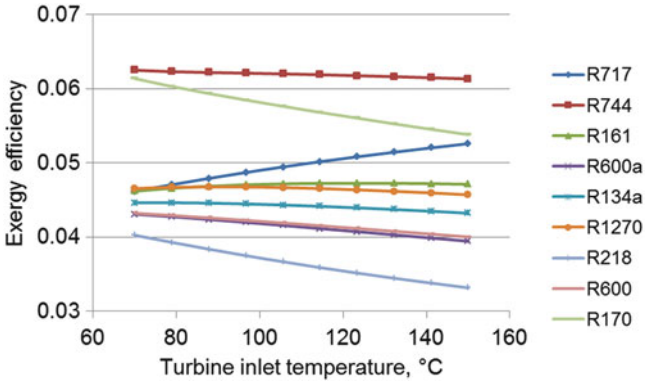

Fig. 15.10 Variation of turbine inlet temperature with exergy efficiency

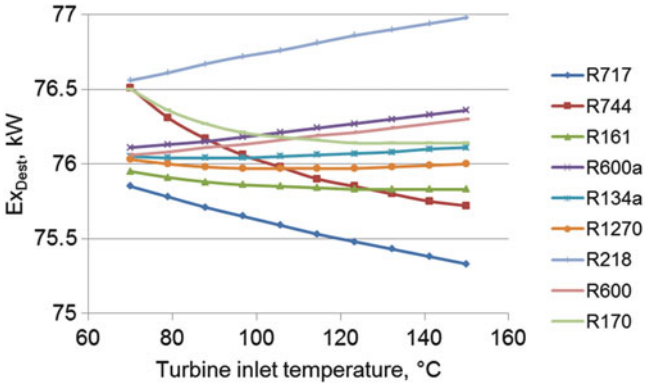

Fig. 15.11 Variation of turbine inlet temperature with exergy destruction rate

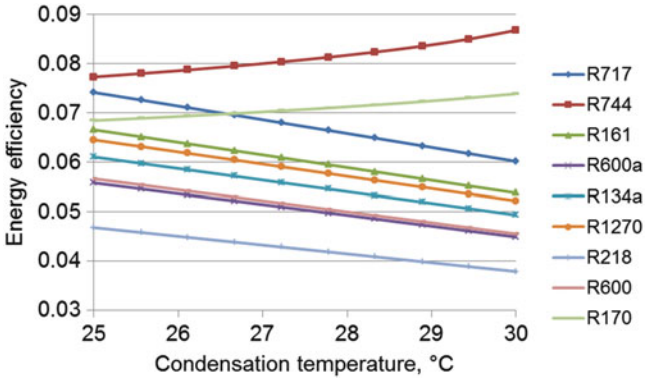

Fig. 15.12 Variation of condensation temperature with energy efficiency

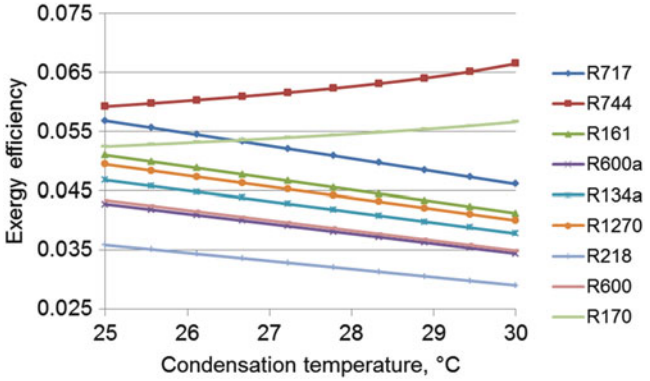

Fig. 15.13 Variation of condensation temperature with exergy efficiency

to energy and exergy efficiency variation. The total exergy destruction rate decreases with increasing the turbine inlet temperature for R1270, R717, R744, R170, it increases for R600a, R134a, R600, R218 and R161.

The condensation temperature is also one of the important parameter for assessment of the system performance. To determine its effect on system performance, it was changed from 25 °C to 30 °C and energy, exergy efficiencies and exergy destruction rates were calculated (Figs. 15.12, 15.13 and 15.14). The results are showed that, the energy and exergetic efficiencies decrease with the increase of the condenser temperature for all working fluids except for R744 and R170. This result is interesting since these two fluids are transcritical fluids. On contrary to this, the total exergy destruction rate increase with the temperature, while for R744 and R170 it decreases.

As declared in Table 15.2 at the beginning of this section, working pressures of solar assisted ORC were determined according to the corresponding saturation

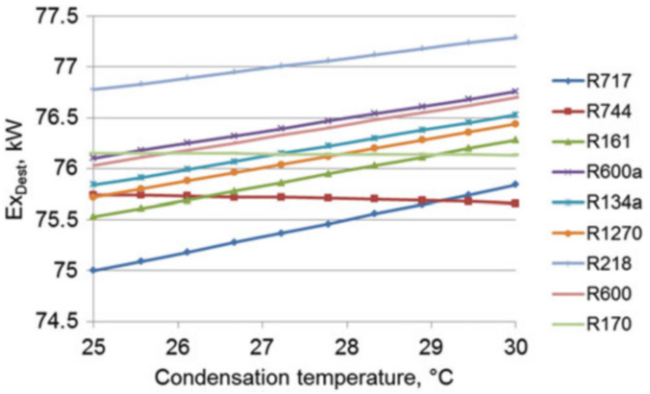

Fig. 15.14 Variation of condensation temperature with exergy destruction rate

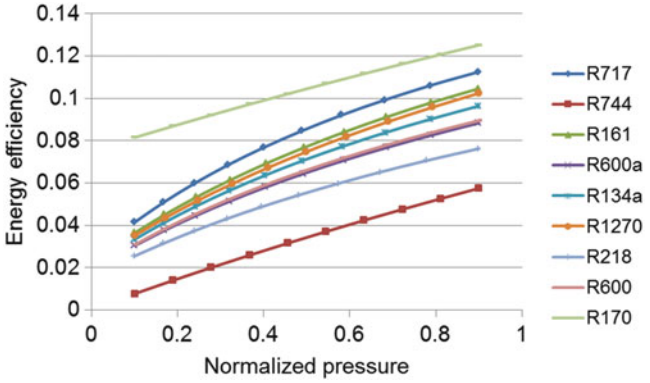

Fig. 15.15 Variation of normalized turbine inlet pressure with energy efficiency

temperatures of evaporator for subcritical working fluids. For transcritical fluids, the pressures were determined from the literature. Since the pressure values of each working fluid differs from each other, they were normalized and the figures were plotted using normalized pressure ranges for better understanding of the results.

Figures 15.15 and 15.16 show the variation of energy and exergy efficiencies with normalized turbine inlet pressure. It is very clear from the figures that with the increase of turbine inlet pressure, efficiencies increase, too.

The effect of normalized turbine inlet pressure on the exergy destruction is given in Fig. 15.17. From the figure, exergy destruction rates decrease with the turbine inlet pressure since the exergy destruction rate is inversely proportional to the energy and exergy efficiencies.

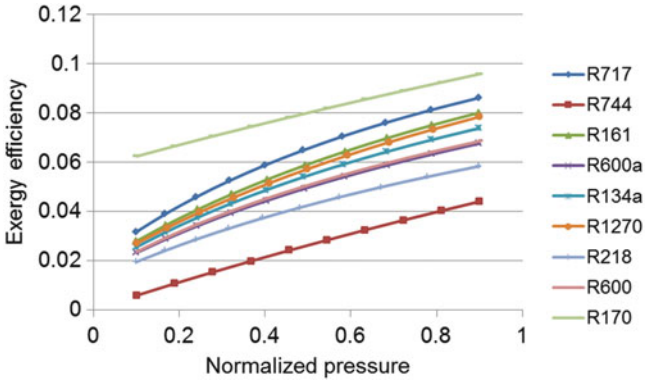

Fig. 15.16 Variation of normalized turbine inlet pressure with exergy efficiency

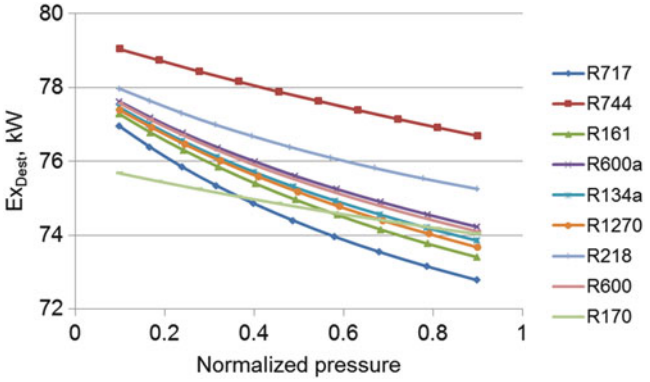

Fig. 15.17 Variation of normalized turbine inlet pressure with exergy destruction rate

Conclusions

A comparative analysis of solar assisted Organic Rankine Cycle for power generation using natural working fluids was investigated. The analyses were carried out for environmentally friendly subcritical and transcritical natural working fluids. The heat energy demand of the ORC was supplied using PTSCs working with Therminol-VP1 as the heat transfer fluid. From the results it was observed that the best cycle performance was obtained using R744 with a power generation rate of 4.87 kW and followed by R170, R717 and R161. Energy analysis results showed that the best cycle had an energy efficiency of 8 % using R744 as working fluid. The exergy efficiency of the same cycle was found to be 7.1 %. The highest total exergy destruction rate was found to be 76.98 kW for R218. Additionally, the effects of turbine inlet temperature, turbine inlet pressure and condensation temperature on

system performance were analysed for different working fluids. This study points out that natural refrigerants are compatible with ORC power generation systems and more detailed experimental studies should be carried out for green energy production assisted by solar energy.

Nomenclature

A_a	Aperture area, m^2
A_g	Glass cover area, m^2
A_r	Receiver area, m^2
Cp	Specific heat, kJ/kg K
D	Tube diameter, m
e	Specific exergy, kJ/kg
$\dot{E}$	Energy, kW
$\dot{E}x$	Exergy, kW
F'	Collector efficiency factor
F_R	Heat removal factor
h	Specific enthalpy, kJ/kg
$h_{c,c-a}$	Convection heat loss coefficient between ambient and the cover, kW/m^2K
$h_{r,c-a}$	Radiation heat transfer coefficient for the glass cover to the ambient, kW/m^2K
h_f	Heat transfer coefficient of fluid inside the tube, kW/m^2K
$h_{r,r-c}$	Radiation heat transfer coefficient between the receiver tube and the glass cover, kW/m^2K
$\dot{m}$	Mass flow rate, kg/s
$\dot{Q}$	Heat, kW
s	Specific entropy, kJ/kg K
$\dot{S}$	Entropy, kW/K
S	Solar irradiation, kW/m^2
T	Temperature, °C or K
U_L	Overall heat loss coefficient, kW/m^2 K
$\dot{W}$	Work, kW
U_0	Overall heat transfer coefficient, kW/m^2 K

Greek Letters

η	Efficiency

Subscripts

dest	Destruction
gen	Generation

i Inlet
o Outlet
u Useful
0 Dead state

References

Al-Sulaiman, F. A. (2013). Energy and sizing analyses of parabolic trough solar collector integrated with steam and binary vapor cycles. *Energy, 58*, 561–570.

Al-Sulaiman, F. A. (2014). Exergy analysis of parabolic trough solar collectors integrated with combined steam and organic Rankine cycles. *Energy Conversion and Management, 77*, 441–449.

ASHRAE. (2004). *Designation and safety classification of refrigerants*. Atlanta, GA: ANSI/ASHRAE Standard 34-2001.

Bejan, A. (1997). *Advanced engineering thermodynamics*. New York: John Wiley and Sons.

Bolaji, B. O., & Huan, Z. (2013). Ozone depletion and global warming: Case for the use of natural refrigerant. *Renewable and Sustainable Energy Reviews, 18*, 49–54.

Calm, J. M., & Hourahan, G. C. (2011). Physical, safety, and environmental data summary for current and alternative refrigerants. In *Proceedings of the 23rd international congress of refrigeration*, Prague, Czech Republic, August 21–26, 2011.

Cengel, Y. A., & Boles, M. A. (2006). *Thermodynamics: An engineering approach* (5th ed.). New York, USA: McGraw-Hill.

Chen, H., Goswami, D. Y., & Stefanakos, E. K. (2010). A review of thermodynamic cycles and working fluids for the conversion of low-grade heat. *Renewable and Sustainable Energy Reviews, 14*, 3059–3067.

Cheng, Z. D., He, Y. L., Cui, F. Q., Xu, R. J., & Tao, Y. B. (2012). Numerical simulation of a parabolic trough solar collector with nonuniform solar flux conditions by coupling FVM and MCRT method. *Solar Energy, 86*, 1770–1784.

Dai, Y., Wang, J., & Gao, L. (2009). Parametric optimization and comparative study of organic Rankine cycle (ORC) for low grade waste heat recovery. *Energy Conversion and Management, 50*, 576–582.

Dincer, I., & Rosen, M. A. (2007). *Exergy: Energy, environment and sustainable development* (1st ed.). Amsterdam: Elsevier Science.

F-Chart, F-Chart Software. Retrieved February 1, 2015, from http://www.fchart.com/.

Franchini, G., Perdichizzi, A., Ravelli, S., & Barigozzi, G. (2013). A comparative study between parabolic trough and solar tower technologies in Solar Rankine Cycle and Integrated Solar Combined Cycle plants. *Solar Energy, 98*, 302–314.

He, C., Liu, C., Gao, H., Xie, H., Li, Y., Wu, S., et al. (2012). The optimal evaporation temperature and working fluids for subcritical organic Rankine cycle. *Energy, 38*, 136–143.

Kalogirou, S. A. (2009). *Solar energy engineering: processes and systems* (1st ed.). Oxford: Academic Press.

Kerme, E. D., & Orfi, J. (2014). Exergy- based thermodynamic analysis of solar driven organic Rankine cycle. *Journal of Thermal Engineering, 33*, 192–202.

Kumar, K. R., & Reddy, K. S. (2009). Thermal analysis of solar parabolic trough with porous disc receiver. *Applied Energy, 86*, 1804–1812.

Lee, Y. R., Kuo, C. R., & Wang, C. C. (2012). Transient response of a 50 kW organic Rankine cycle system. *Energy, 48*, 532–538.

Maraver, D., Royo, J., Lemort, V., & Quoilin, S. (2014). Systematic optimization of subcritical and transcritical organic Rankine cycles (ORCs) constrained by technical parameters in multiple applications. *Applied Energy, 117*, 11–29.

Peris, B., Navarro-Esbri, J., Moles, F., Collado, R., & Mota-Babiloni, A. (2015). Performance evaluation of an organic Rankine cycle for power applications from low grade heat sources. *Applied Thermal Engineering, 75*, 763–769.

Petela, R. (2005). Exergy analysis of the solar cylindrical-parabolic cooker. *Solar Energy, 79*, 221–233.

Refrigerants naturally, C/O Heat International. Retrieved February 2, 2015, from http://www.refrigerantsnaturally.com/.

Restrepo, G., Weckert, M., Brüggemann, R., Gerstmann, S., & Frank, H. (2008). Ranking of refrigerants. *Environmental Science & Technology, 42*, 2925–2930.

Shengjun, Z., Huaixin, W., & Tao, G. (2011). Performance comparison and optimization of subcritical ORC and transcritical power cycle system for low-temperature geothermal power generation. *Applied Energy, 88*, 2740–2754.

Tchanche, B. F., Lambrinos, G., Frangoudakis, A., & Papadakis, G. (2011). Low-grade heat conversion into power using organic Rankine cycles—A review of various applications. *Renewable and Sustainable Energy Reviews, 15*, 3963–3979.

Therminol, Heat transfer fluids by Eastman. Therminol VP-1. Retrieved December 10, 2014, from http://www.therminol.com/products/Therminol-VP1.

Tiwari, G. N. (2003). *Solar energy: Fundamentals, design, modelling and applications*. Pangbourne: Alpha Science International Ltd.. 525 p.

Vélez, F., Segovia, J., Chejne, F., Antolin, G., Quijano, A., & Martín, M. C. (2011). Low temperature heat source for power generation: Exhaustive analysis of a carbondioxide transcritical power cycle. *Energy, 36*, 5497–5507.

Vogel, T., Oeljeklaus, G., Görner, K., Dersch, J., & Polklas, T. (2014). Hybridization of parabolic trough power plants with natural gas. *Energy Procedia, 49*, 1238–1247.

Volker. Retrieved January 14, 2015, from http://www.volker-quaschning.de/articles/fundamentals2/index_e.php.

Wang, M., Wang, J., Zhao, Y., Zhao, P., & Dai, Y. (2013). Thermodynamic analysis and optimization of solar-driven regenerative ORC based on flat-plate solar collectors. *Applied Thermal Engineering, 50*, 816–825.